Flux-assisted synthesis of tungsten doped layered perovskite oxychloride with promoted visible-light-responsive O_2 evolution performance

Xiangyao Song,[+[a]] Shiwen Du,[+[b]] Xiangying Xing,[+[a]] Beibei Dong,[*[a]] Zhaochi Feng,[[b]] Fei Cheng[*[a]]

[a] School of Chemistry and Chemical Engineering, Hebei University of Technology, Tianjin 300130, China

[b] Dalian Institute of Chemical Physics, Chinese Academy of Sciences, Dalian 116023, China.

E-mail: bbdong@hebut.edu.cn

E-mail: fcheng@hebut.edu.cn

[+] X. Song, S. Du, and X. Xing contributed equally.

Experimental

Chemicals

Bi_2O_3 (99.9%), $BaCO_3$ (99.95%), NaCl (99.8%), $ZrCl_4$ (98%), Y_2O_3 (99.99%), and $La(NO_3)_3 \cdot 6H_2O$ (99.99%) were provided by Shanghai Aladdin Bio-Chem Technology Co., Ltd. BiOCl (99%), WCl_6 (99.5%), $Ti(SO_4)_2$ (≥ 96%), and $ZnSO_4 \cdot 7H_2O$ (99.5%) were obtained from Shanghai Macklin Biochemical Co., Ltd. Ta_2O_5 (99.99%) was provided by Mlbio Co., Ltd. (Shanghai, China). KCl (99.5%) was obtained from Sinopharm Chemical Reagent Co., Ltd. $AgNO_3$ (99.995%) was provided by Alfa Aesar. Deionized water (UPR-II-10T, Wuhan Ulupure Pure Water Equipment Co., Ltd.) was used in the whole experiment.

Synthesis

For the preparation of pristine $Ba_2Bi_3Ta_2O_{11}Cl$ (labelled as BBTOC), 0.358 g Bi_2O_3, 0.303 g $BaCO_3$, 0.339 g Ta_2O_5, and 0.21 g BiOCl (molar ratios of Bi_2O_3:$BaCO_3$:Ta_2O_5:BiOCl = 1:2:1:1.05 and an excess of 5% BiOCl is used to compensate the chlorine loss of volatilization at high temperature) were ground in an agate mortar for 1.5 h. Thereafter, the mixture was calcined in a corundum crucible (30 mL) for 20 h at 1073 K with a heating rate of 10 K/min. Subsequently, the system was naturally cooled to room temperature, and then the obtained product was rinsed with hot water for three times (353 K, 0.6 L in total) to remove the excess flux. Finally, the yellow product was dried in an oven at 353 K for 12 h.

The preparation of BBTOC treated with molten salt (labelled as BBTOC-F) are similar with the above-mentioned procedures except that the mixture was further

ground with NaCl and KCl (molar ratios of BBTOC:NaCl:KCl = 1:10:10) for 20 min.

For the preparation of W-doped BBTOC-F (labelled as W-BBTOC-F), 0.009/0.018/0.027 g WCl_6 is added in the above-mentioned grinding process (molar ratios of W/BBTOC = 3%/6%/9%). For the preparation of BBTOC-F doped with other metals, the similar procedures are employed and 0.011 g $ZrCl_4$, 0.011 g $Ti(SO_4)_2$, 0.005 g Y_2O_3, 0.013 g $ZnSO_4 \cdot 7H_2O$, or 0.020 g $La(NO_3)_3 \cdot 6H_2O$ are added with the molar ratios of metal/BBTOC = 6%.

Photocatalytic reaction

The photocatalytic O_2 evolution reaction was conducted in a closed circulation system (laboratory solar-6A, Beijing Perfect Light Co., Ltd.) equipped with a top radiation reaction vessel. The reaction solution was irradiated (i = 20 A, and $\lambda \geq 420$ nm) with a 300 W Xe lamp (CEL-HXF300H5, Beijing Perfectlight Technology Co., Ltd.), and the obtained gas was analyzed by the online GC-2014 gas chromatography (Shimadzu Corporation). 0.05 g photocatalyst was uniformly scattered in the aqueous solution after ultrasonic treatment, and then vacuumized for 20 min to ensure that the air was completely removed before irradiation. The silver nitrate (5 mM) was used as the electron sacrificial reagent in the O_2-evolving reaction.

Photoelectrochemical (PEC) measurement

The drop-casting method was employed to prepare the BBTOC electrodes. 20 mg powder was dispersed in 5 mL isopropanol and sonicated for 2 h. Thereafter, the solution was dropped on the surfaces of fluorine-doped tin oxide glass (FTO, 1 × 2 cm^2), and the obtained electrodes were naturally dried in air and calcined in a muffle

furnace at 773 K for 30 min.

The CHI660E workstation was employed in the (photo)electrochemical tests using a three-electrode system (Pt counter and calomel reference electrodes). A 0.5 M aqueous sodium sulfate solution (pH = 8 adjusted by sodium hydroxide) was used as the electrolyte. The AC potential amplitude and frequency of Mott–Schottky test were 5 mV and 10 kHz, and the AC potential and frequency of electrochemical impedance spectroscopy (EIS) test were set as 1.2 V (vs. NHE) and 0.1-100 kHz, respectively. The PEC current was obtained at a scanning rate of 3 mV/s under visible light irradiation (i = 20 A, and $\lambda \geq 420$ nm).

Material characterization

The crystalline structures of the samples were studied by X-ray diffractometry (XRD, D8 Discover, Bruker). The high-resolution transmission electron microscopy (HRTEM) and scanning electron microscopy (SEM) images were measured using Talos F200S and Quanta 450 FEG, respectively. The ESCALAB 250Xi system was employed to obtain X-ray photoelectron spectroscopy (XPS) spectra. Ultraviolet-visible diffuse reflectance spectroscopy (UV–vis DRS) was collected on an ultraviolet-visible-near-infrared spectrophotometer (Varian Cary 500) equipped with an integrating sphere, and $BaSO_4$ was used as the reflectance standard. The photoluminescence (PL) spectrum was measured by fluorescence spectrophotometer (FSP920), and the excitation wavelength was 242 nm.

Calculations

All the density functional theory (DFT) calculations were performed using the

Vienna ab initio simulation package (VASP)[1], which was based on the projected augmented wave (PAW)[2] pseudo potential with a cut-off energy of 500 eV. The generalized gradient approximation (GGA)[3] with Perdew-Burke-Ernzerhof (PBE)[4] functional was used to approximate the exchange and correlation effects in the relaxation process. In the process of structural optimization, set the convergence criterion of energy on each atom to 1.0×10^{-5} eV, and set the force convergence threshold of each atom to 0.015 eV·Å^{-1}. The models of BBTOC (001) slab (constructed from BBTOC 3 × 3 × 1 supercell including 18 Ba atoms, 27 Bi atoms, 18 Ta atoms, 99 O atoms, and 9 Cl atoms) and W-doped BBTOC (001) slab (including 18 Ba atoms, 27 Bi atoms, 17 Ta atoms, 1 W atom, 99 O atoms, and 9 Cl atoms) were built with a vacuum spacing of 15 Å to simulate the OER pathway using a Monkhorst-Pack[5] grids of 2 × 2 × 1, and the reaction mechanism is expressed as the following Equations (1-4):

$$H_2O + * \rightarrow *OH + H^+ + e^- \quad (1)$$

$$*OH \rightarrow *O + H^+ + e^- \quad (2)$$

$$*O + H_2O \rightarrow *OOH + H^+ + e^- \quad (3)$$

$$*OOH \rightarrow * + O_2 + H^+ + e^- \quad (4)$$

where, the asterisk (*) refers to an active surface site, and *OH, *O, and *OOH denote the adsorbed intermediates, respectively. The Gibbs free energies of the OER process were evaluated as Equation (5):

$$G = E_{DFT} + E_{ZPE} - TS \quad (5)$$

where, E_{DFT}, E_{ZPE}, and TS represent DFT-calculated electronic energy, zero-point energy, and entropy of the system, respectively.

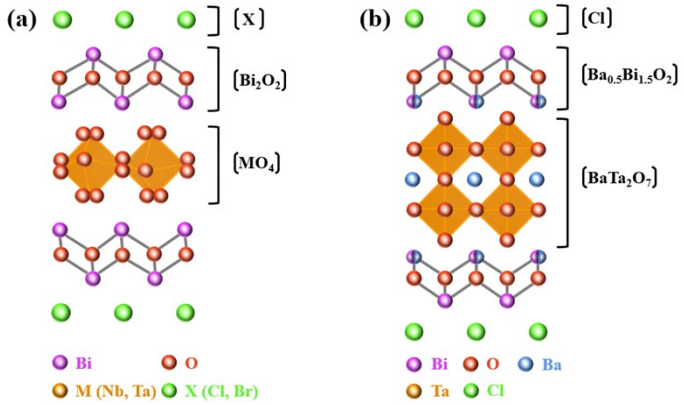

Fig. S1 Crystal structures of Sillén-Aurivillius layered oxyhalides of (a) single-layered (n = 1) Bi_4MO_8Cl and (b) double-layered (n = 2) BBTOC.

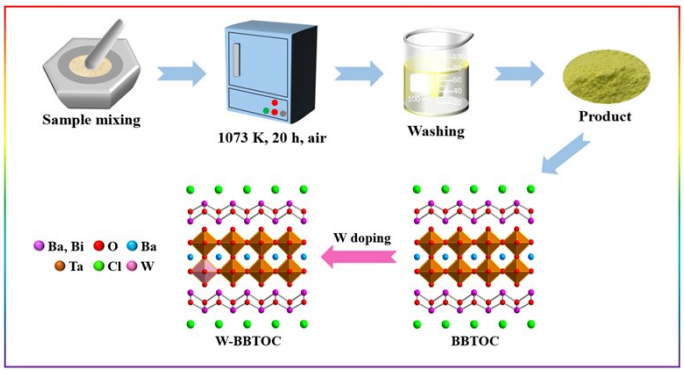

Fig. S2 Schematic diagram of the preparation of the typical samples.

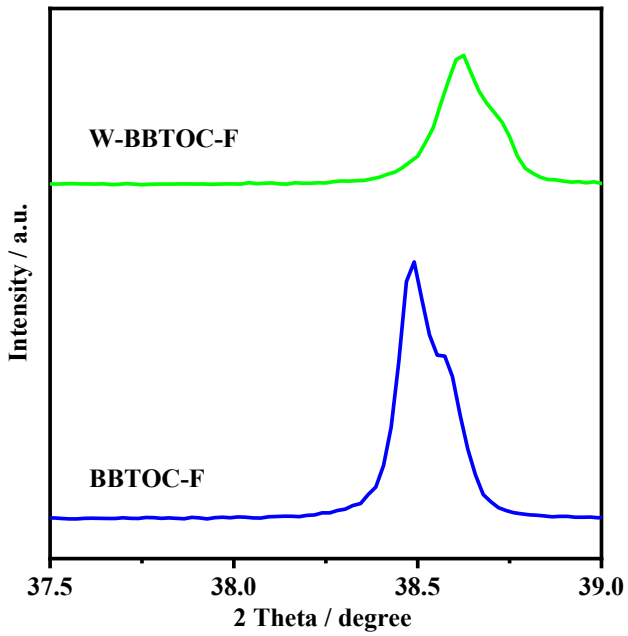

Fig. S3 The enlarged XRD patterns of BBTOC-F and W-BBTOC-F.

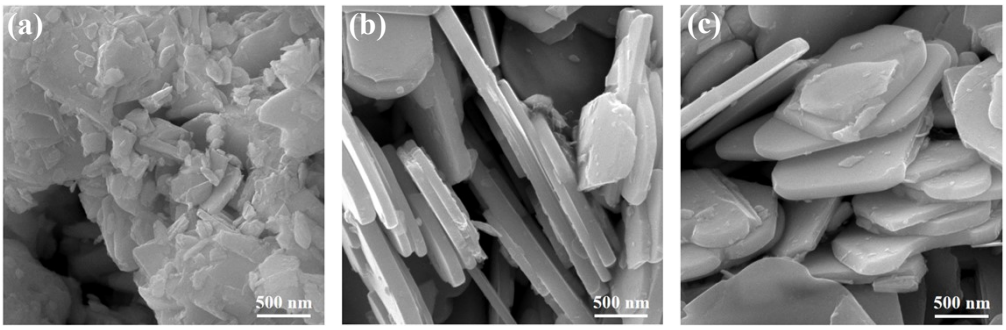

Fig. S4 SEM images of BBTOC (a), BBTOC-F (b), and W-BBTOC-F (c).

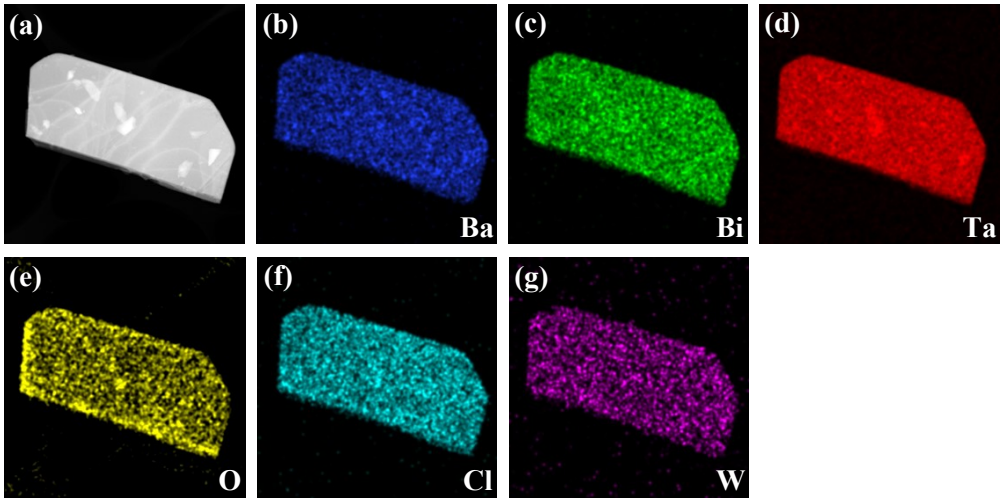

Fig. S5 EDS mapping images of the typical elements of W-BBTOC-F (a): Ba (b), Bi (c), Ta (d), O (e), Cl (f), and W (g).

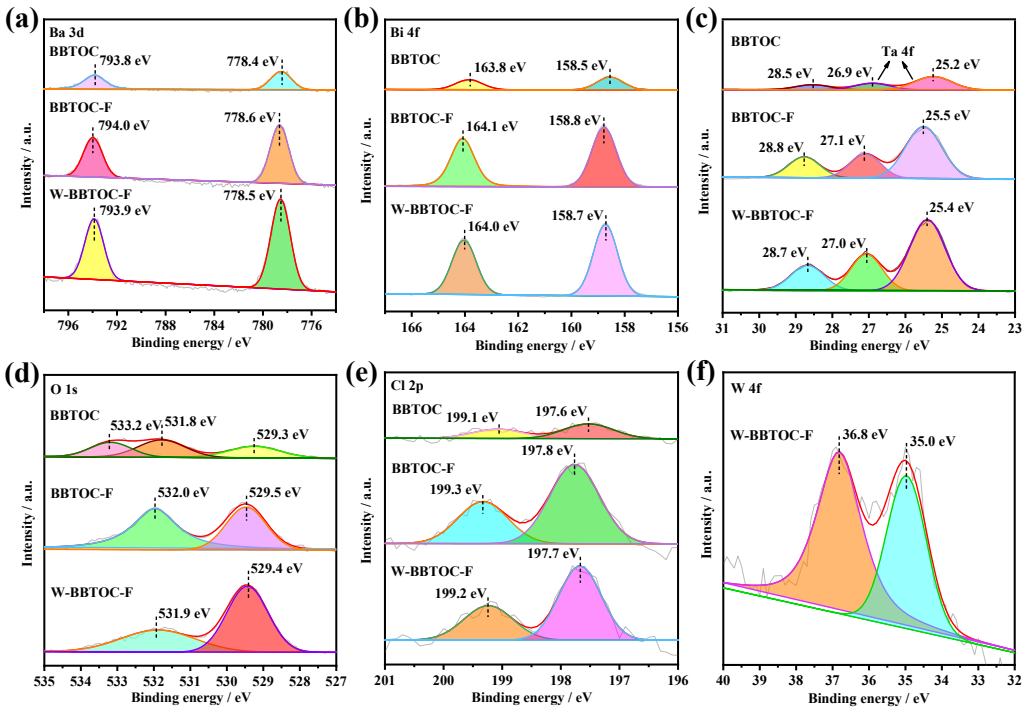

Fig. S6 XPS spectra of the three typical samples: Ba 3d (a), Bi 4f (b), Ta 4f (c), O 1s (d), Cl 2p (e), and W 4f (f).

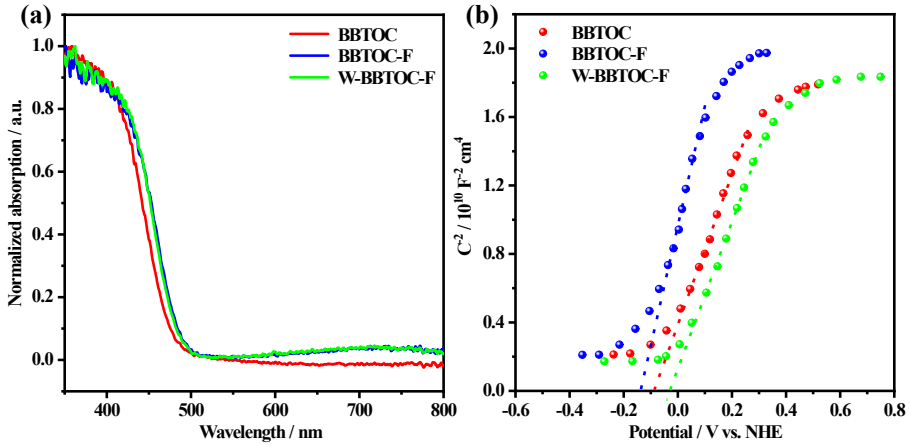

Fig. S7 UV–vis DRS (a) and Mott–Schottky curves (b) of the three typical samples. The following formula is generally employed to calculate the charge carrier density:

$$N_d = \frac{2}{A^2 e_0 \epsilon \varepsilon_0}\left[d\left(\frac{1}{c^2}\right)\Big/ dV\right]^{-1}$$

where A is the electrode area (1 cm^2 in this study), $^{e}{}_{0}$ is the electronic charge, ϵ and

ε_0 is the dielectric constant of the catalyst and vacuum, respectively, V is the potential applied to the electrode, and N_d is the carrier density. It can be observed that the positive slope of Mott-Schottky curve of W-BBTOC-F is lower than that of BBTOC-F, demonstrating that the charge carrier density of W-BBTOC-F is higher, thus promoting the charge separation.[6]

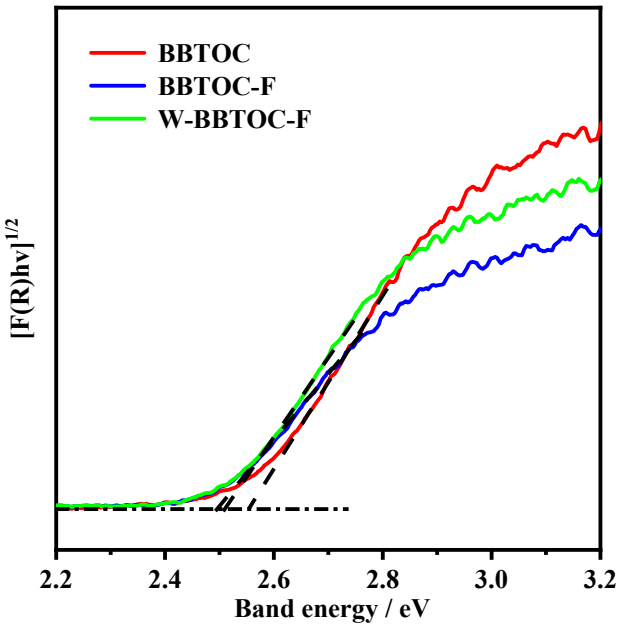

Fig. S8 Tauc plots of the three typical samples.

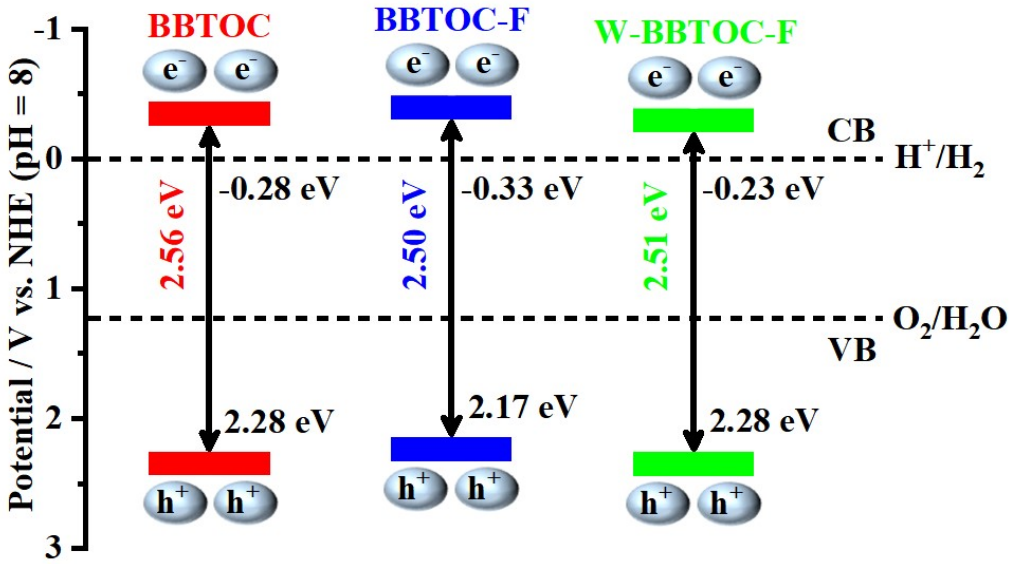

Fig. S9 Schematic illustration of the energy band structures of the three typical

samples.

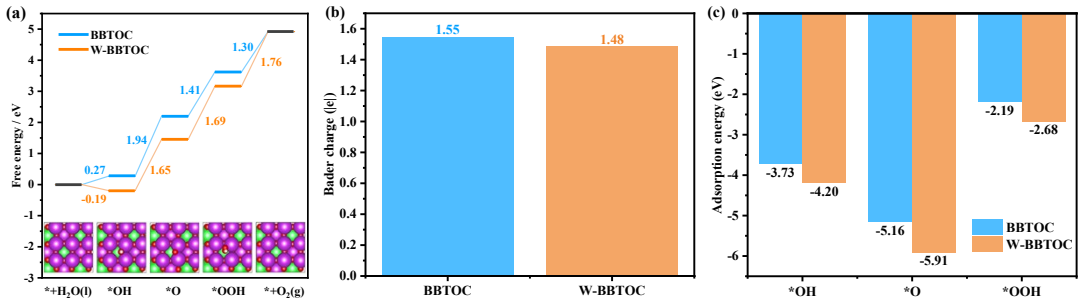

Fig. S10 Calculated free energy diagrams for the four basic water oxidation steps of the BBTOC and W-doped BBTOC models (a), Bader charge analysis of surface Bi ions (b), and adsorption energy of the corresponding species (c). Basically, the electronic structure of the material fundamentally governed their binding strength with surface absorbed species and thus the Gibbs free energies can be altered. The Bader charge analysis of surface Bi ions shows that the partial charge decreases from ~1.55 to 1.48 for the Bi atom after W doping (Fig. S10b), indicating the strong electronic interaction between W and Bi. Moreover, the W-doped BBTOC provides stronger oxygen binding strength compared with the original Bi site in pristine BBTOC (Fig. S10c), which is beneficial for weakening the H−O bond, reducing the energy barrier of the rate-limiting step, and finally improving the OER performance.[7]

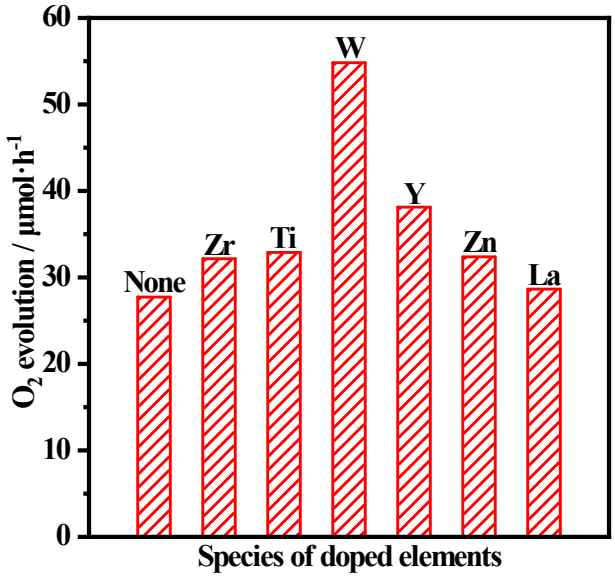

Fig. S11 Photocatalytic O_2 production activities of the BBTOC-F doped with different metal ions with the same doping concentration (molar ratios of metal/BBTOC = 6%) under visible light irradiation (i = 20 A, and $\lambda \geq 420$ nm).

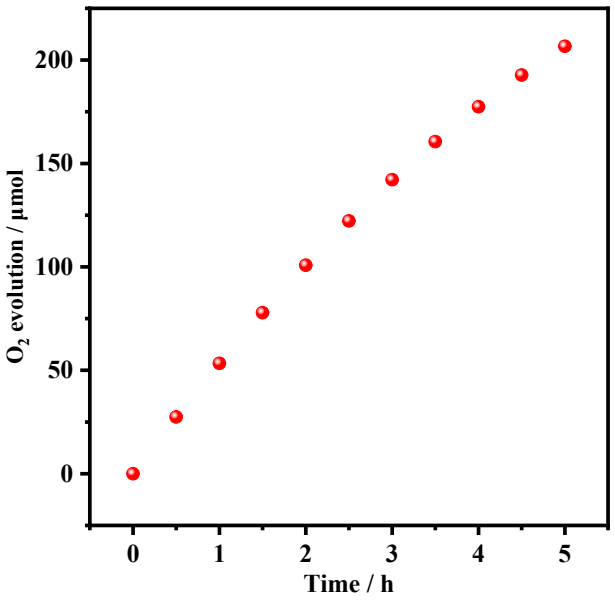

Fig. S12 The long-term cyclic curve of the photocatalytic O_2 production of W-BBTOC-F.

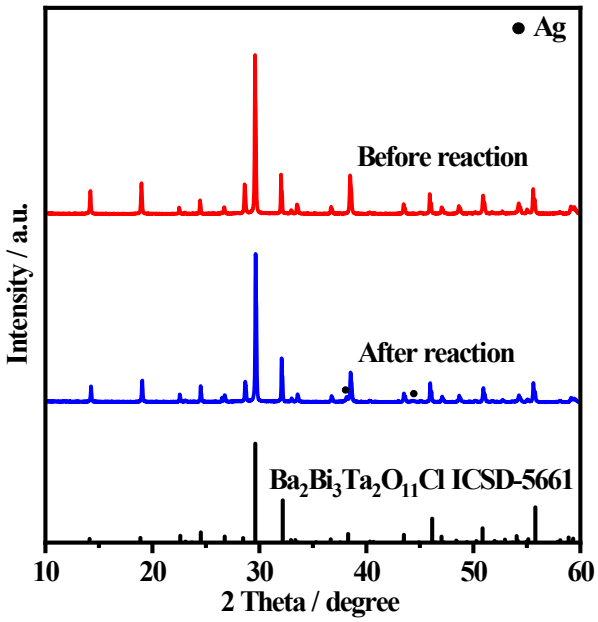

Fig. S13 XRD patterns of W-BBTOC-F before and after the long-term O_2 evolution reaction.

References

1 G. Kresse and D. Joubert, *Phys. Rev. B*, 1999, **59**, 11–19.

2 P. E. Blöchl, *Phys. Rev. B*, 1994, **50**, 17953–17979.

3 J. P. Perdew, K. A. Jackson, M. R. Pederson, D. J. Singh and C. Fiolhais, *Phys. Rev. B*, 1992, **46**, 11–15.

4 J. P. Perdew, K. Burke and M. Ernzerhof, *Phys. Rev. Lett.*, 1996, **77**, 3865–3868.

5 H. J. Monkhorst and J. D. Pack, *Phys. Rev. B*, 1976, **13**, 5188–5192.

6 X. Zhao, J. Hu, S. Chen and Z. Chen, *Phys. Chem. Chem. Phys.*, 2018, **20**, 13637-13645.

7 J. Sun, H. Xue, Y. Zhang, X. L. Zhang, N. Guo, T. Song, H. Dong, Y. Kong, J. Zhang and Q. Wang, *Nano Lett.*, 2022, **22**, 3503-3511.